Electronic Supplementary Material (ESI) for Nanoscale Advances.

Supplementary Information for

Electrostatic Control of Excitonic Photoluminescence from Both A and B Excitons in Monolayer Molybdenum Disulfide

Yuchun Liu, Tianci Shen, Shuangyi Linghu, Ruilin Zhu and Fuxing Gu*

S1. CVD Synthesis of monolayer MoS_2

Monolayer MoS_2 on the Si/SiO_2 substrate was grown by using CVD technique in the a furnace with double temperature zones. As shown in Fig. S1(a), two alumina boats with sulfur powder (S, ≥99.5%) and molybdenum (VI) oxide (MoO_3, ≥99%) powder were placed upstream and downstream of the two-zone furnace, respectively. Several SiO_2/Si substrates (dimensions of 10 mm × 50 mm × 1 mm) were placed faced-down on the MoO_3 boat. The temperatures of two-zone furnace were controlled by heating-set system program. High-purity argon gas (Ar) was introduced into the quartz tube with a flow rate of 100~200 sccm during the growth process. The growth temperature was set to 850~870 °C and growth time was about 10~20 minutes for monolayer MoS_2 in our growth system at an nearly atmospheric pressure. The monolayer MoS_2 flakes with different quality can be achieved through changing the Mo:S ratio of precursor and the gas flow rate. For the growth of S-rich monolayer MoS_2, 200 mg sulfur powder and 5 mg MoO_3 powder were used as precursors with an Ar flow rate of 100 ~ 150 sccm. For the growth of Mo-rich monolayer MoS_2, 200 mg sulfur powder and 10 mg MoO_3 powder were used as precursors, and the Ar gas flow rate was 150 sccm. Fig. S1(b−c) shows the optical microscopy images of the CVD-grown S-rich and Mo-rich monolayer MoS_2 on SiO_2/Si substrates.

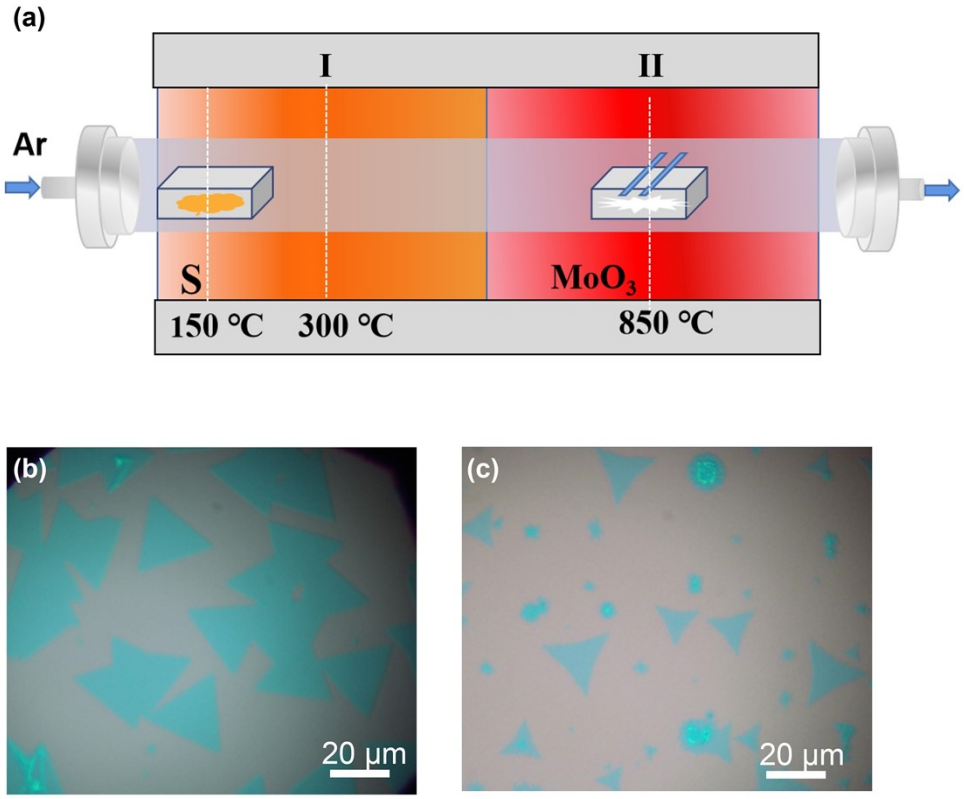

Fig. S1 (a) Setup schematic diagram for the monolayer MoS_2 growth by CVD method in a two-zone furnace; (b–c) Optical microscopy image of the CVD-grown S-rich and Mo-rich monolayer MoS_2 on SiO_2/Si substrates.

S2. Morphology and surface potential of S-rich and Mo-rich monolayer MoS_2

The morphology, surface potential mapping and line profiles for the monolayer MoS_2 samples with Au electrode on SiO_2/Si substrate are shown in Fig. S2. The contact potential difference (CPD) of MoS_2 was measured with the Scanning Kelvin Probe in air ambient. In principle, the measured CPD is the difference in work function between the sample surface and the probe: $eV_{CPD} = \Phi_{tip} - \Phi_{sample}$, where ϕ_{tip} is the known work function of reference tip and ϕ_{sample} is the work function of the sample. To investigate the surface potential difference of different MoS_2 on Si/SiO_2 substrate, Au films with a thickness of ~40 nm were used as references. The measured surface potential difference between the S-rich MoS_2 monolayer and Au was ~–44 mV, while that between Mo-rich MoS_2 and Au was ~52 mV. It indicted that the S-rich MoS_2 exhibited a higher work function and lower electron density than that of the Mo-rich MoS_2.

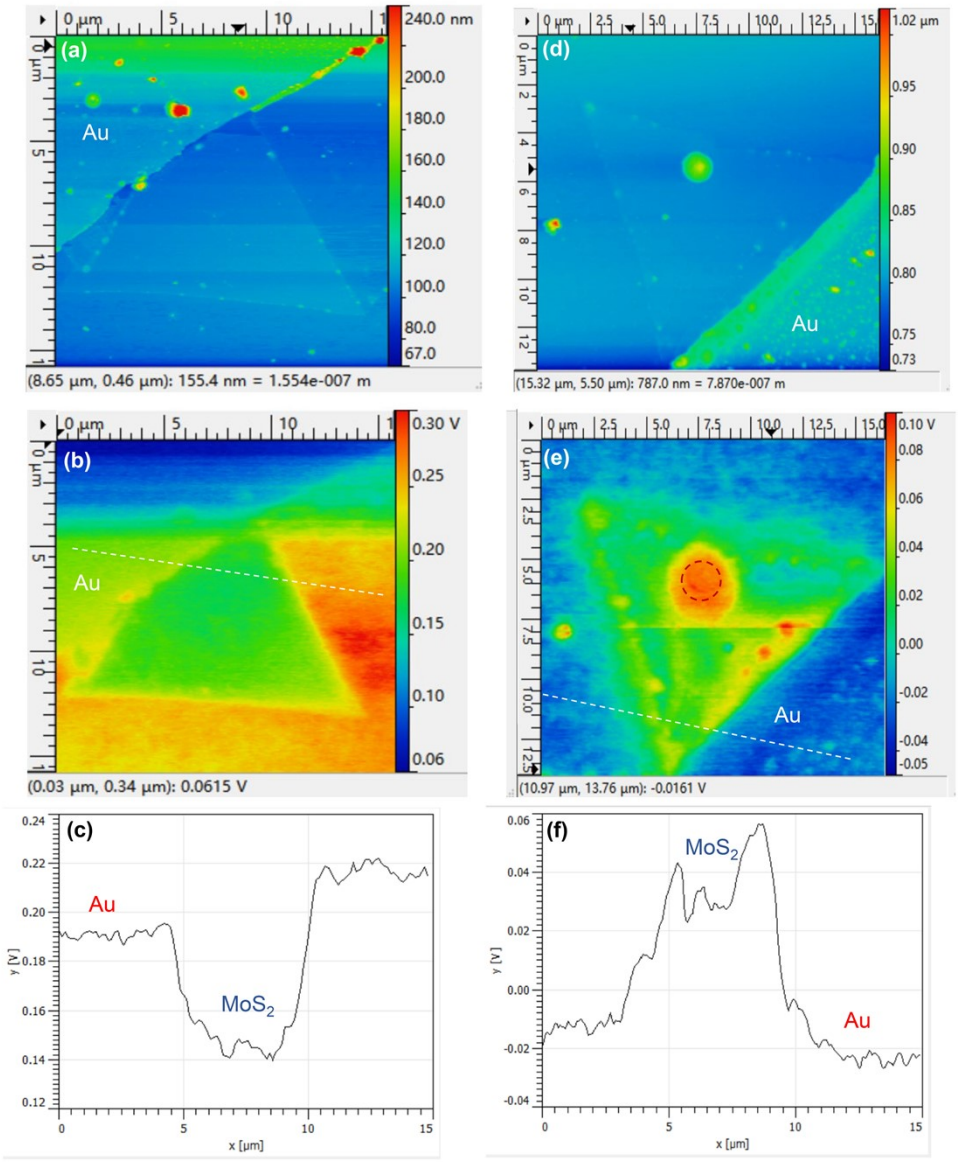

Fig. S2 Morphology, surface potential mapping and line profiles for the monolayer MoS_2 samples with Au electrode on SiO_2/Si substrate: (a–c) S-rich and (c-d) Mo-rich MoS_2.

It should be noted that the laser power intensity was $<10^3$ W/cm^2 for PL and Raman spectra measurements. Since the collection time for measurement of each spectra is very short (<30 seconds), there no obvious structure defects induced by the laser irradiation in the monolayer MoS_2. Only when the laser excitation last for a long time, additional structure defects can be produced[1]. As shown in Fig. S2 (e), the red dash circles represented the region of continuous laser irradiation for 30 minutes on MoS_2 with laser power intensity of 2.4×10^3 W/cm^2 (three times as the power intensity for PL measurements). The continuous laser irradiation led to an increase of 40~50 mV in the V_{CPD} for the Mo-rich MoS_2, which inferred an increase of defect density and a decrease of work function.

S3. Statistical PL intensity ratio for the S-rich and Mo-rich monolayer MoS_2

The statistical data were obtained from more than 10 tests of PL spectra for the S-rich and Mo-rich MoS_2 samples, which are similar to that in Fig. 3 and Fig. 4. The estimated statistical value of PL intensity ratio for both the S-rich and Mo-rich MoS_2 with the error bars are shown in Fig. S3.

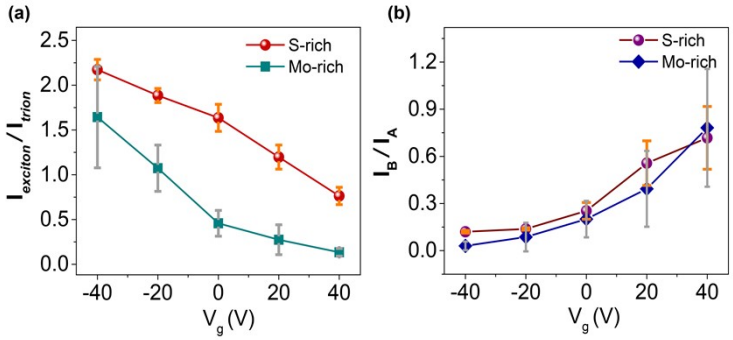

Fig. S3 Statistical PL intensity ratio for the S-rich and Mo-rich MoS_2: (a) $I_{exciton}/I_{trion}$, (b) I_B/I_A

S4. Statistical PL intensity ratio for the S-rich and Mo-rich monolayer MoS_2

The S-rich MoS_2 sample on SiO_2/Si was doped by spin-coating PEDOT:PSS and was dried naturally in air. After doped by PEDOT:PSS, the sulfur vacancies can be healed spontaneously by the sulfur adatom clusters through a PSS-induced hydrogenation[2]. The PL emission were measured under the same condition as that of the S-rich and Mo-rich monolayer MoS_2. Fig. S4 shows the PL spectra and integrated PL intensity of different excitons (A^0, A^- and B) at different V_g. After PEDOT:PSS spin coating on the CVD-grown MoS_2, the trion PL of doped MoS_2 showed a weak dependence on V_g, similar to the observation of a PL less sensitive to V_g in the reported works.

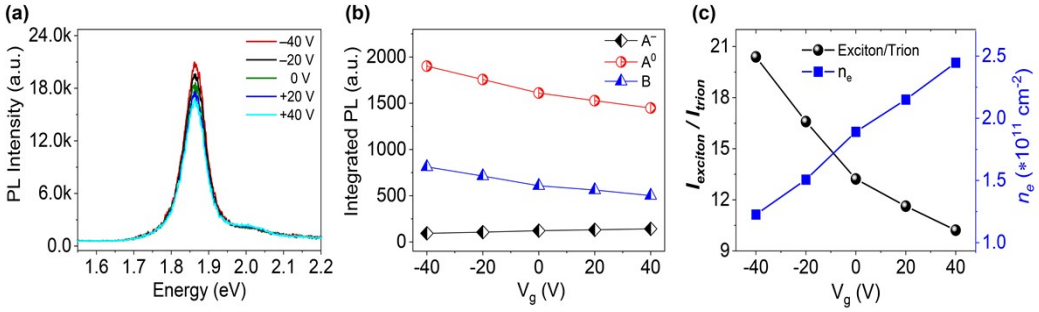

Fig. S4 Gate-dependent PL properties of the S-rich monolayer MoS_2 sample after PEDOT:PSS doping: (a–b) PL spectra and integrated PL intensity of A^0, A^-, and B excitons; (c) $I_{exciton}/I_{trion}$ ratio versus V_g, and calculated electron density versus V_g.

References

[1] H. M. Oh, G. H. Han, H. Kim, J. J. Bae, M. S. Jeong and Y. H. Lee, *ACS Nano*, 2016, **10**, 5230–5236.

[2] X. Zhang, Q. Liao, S. Liu, Z. Kang, Z. Zhang, J. Du, F. Li, S. Zhang, J. Xiao, B. Liu, Y. Ou, X. Liu, L. Gu and Y. Zhang, *Nature Commun.*, 2017, **8**, 15881.